

Spatial and temporal regulation of ventral spinal cord precursor specification by Hedgehog signaling

Hae-Chul Park*, Jimann Shin* and Bruce Appel†

Department of Biological Sciences, Vanderbilt University, Nashville, TN 37235, USA

*These authors contributed equally to this work

†Author for correspondence (e mail: b.appel@vanderbilt.edu)

Accepted 22 September 2004

Development 131, 5959-5969
Published by The Company of Biologists 2004
doi:10.1242/dev.01456

Summary

Graded Hedgehog (Hh) signaling patterns the spinal cord dorsoventral axis by inducing and positioning distinct precursor domains, each of which gives rise to a different type of neuron. These domains also generate glial cells, but the full range of cell types that any one precursor population produces and the mechanisms that diversify cell fate are unknown. By fate mapping and clonal analysis in zebrafish, we show that individual ventral precursor cells that express *olig2* can form motoneurons, interneurons and oligodendrocytes. However, *olig2*⁺ precursors are not developmentally equivalent, but instead produce subsets of progeny cells in a spatially and temporally biased manner.

Using genetic and pharmacological manipulations, we provide evidence that these biases emerge from Hh acting over time to set, maintain, subdivide and enlarge the *olig2*⁺ precursor domain and subsequently specify oligodendrocyte development. Our studies show that spatial and temporal differences in Hh signaling within a common population of neural precursors can contribute to cell fate diversification.

Key words: Oligodendrocytes, Motoneurons, Hedgehog, Zebrafish, Neural precursor, Spinal cord

Introduction

Throughout the nervous system of vertebrate embryos, proliferative neuroepithelial precursors give rise first to neurons and, later, glial cells. For example, a common population of precursors, called pMN, that occupies the ventral spinal cord produces motoneurons and then oligodendrocyte progenitor cells (OPCs), which form oligodendrocytes, the myelinating cell type of the central nervous system (CNS) (Richardson et al., 2000; Rowitch, 2004). Precursors that occupy more dorsal regions of the spinal cord appear to similarly switch from neuronal to glial cell production, generating interneurons and astrocytes (Pringle et al., 2003; Stolt et al., 2003; Zhou and Anderson, 2002). The switch between neuronal and glial production plays a crucial role in building functional nervous systems, yet the mechanisms that regulate it are poorly understood.

In amniotes, pMN precursors express *Olig1* and *Olig2*, which encode basic helix-loop-helix (bHLH) transcription factors (Lu et al., 2000; Takebayashi et al., 2000; Zhou et al., 2000) and *Olig* gene functions are required for motoneuron and oligodendrocyte development (Lu et al., 2002; Park et al., 2002; Takebayashi et al., 2002; Zhou and Anderson, 2002). A single *Olig* gene, *olig2*, is similarly expressed in ventral spinal cord of zebrafish and necessary for primary motoneuron and OPC formation (Park et al., 2002). A morphogenetic gradient of sonic hedgehog (Shh), which originates from notochord (mesoderm that underlies the ventral spinal cord) and floor plate (the ventral-most spinal cord cell type), establishes the *Olig* expression domain and, thus, pMN precursors (Jessell,

2000; Poh et al., 2002; Shirasaki and Pfaff, 2002). A subset of *Olig*⁺ cells express neurogenin (*Ngn*) genes (Mizuguchi et al., 2001; Novitch et al., 2001; Park and Appel, 2003; Zhou et al., 2001), which also encode bHLH transcription factors, during the period of motoneuron production. *Ngn* expression subsides in ventral spinal cord cells at about the time that production of motoneurons ends and formation of OPCs begins (Zhou et al., 2001). Additionally, overexpression experiments showed that *Olig2* and *Ngn2* together can promote motoneuron development (Mizuguchi et al., 2001; Novitch et al., 2001). These observations raised the possibility that differential bHLH protein expression creates a combinatorial code wherein cells that express both *Olig2* and *Ngn2* develop as motoneurons and those that express only *Olig2*, following *Ngn2* downregulation, develop as OPCs (Zhou and Anderson, 2002; Zhou et al., 2001). However, the precise mechanisms that regulate specification of pMN precursors for different fates are not clear.

Here, we address the following questions. First, are pMN cells specified only for motoneuron and OPC fates or do they also give rise to other cell types? Second, can an individual pMN precursor give rise to various progeny or does each precursor produce only a single kind of daughter cell? Finally, what are the molecular signals that promote OPC development from pMN precursors? We show that individual pMN precursors produce a variety of distinct cell types in a manner that is independent of lineage, but spatially and temporally biased. Differences in neural cell response to Hh signaling create these biases, which are necessary for OPC development.

Materials and methods

Wild-type, mutant and transgenic zebrafish

Embryos were raised at 28.5°C and staged according to hours post-fertilization (hpf), days post-fertilization (dpf) and morphological criteria (Kimmel et al., 1995). Mutant and transgenic alleles included *smu^{b641}* (Barresi et al., 2000; Varga et al., 2001), *syu^{t4}* (Schauerte et al., 1998), *Tg[olig2:egfp]^{vu12}* and *Tg[olig2:egfp]^{vu13}* (Shin et al., 2003).

Single cell labeling

Transgenic embryos at 90% epiboly stage were dechorionated with pronase (5 mg/ml, Sigma) for 10 minutes and rinsed twice with embryo medium (EM) (Westerfield, 2000). Bud stage (10 hpf) embryos were mounted, dorsal side upwards, in 3% methyl cellulose (1500 centipoises, Sigma) submerged in EM on a depression slide. Intracellular dye labeling was performed essentially as described previously (Eisen et al., 1989), targeting the posterior *olig2:EGFP⁺* domain (see Fig. S1 in the supplementary material). By inspecting embryos at multiple focal planes and from different angles, we determined whether one or more cells were labeled. Greater than 70% of injected embryos were rejected because more than one cell was filled with dye. Embryos with single labeled cells were transferred individually to EM with 0.5% penicillin/streptomycin (Gibco) in 24-well plates and raised in the dark at 28.5°C. At 2.5 dpf, labeled cells were analyzed using a Zeiss LSM510 Meta laser scanning confocal microscope. All clones occupied positions between somites 6 and 15.

BrdU labeling and immunohistochemistry

Thirty-six hpf embryos were incubated in a 0.5% solution of BrdU (Roche) in EM for 12 hours at 28.5°C and processed as described previously (Park and Appel, 2003). For immunohistochemistry, we used the following primary antibodies: mouse anti-BrdU (G3G4, 1:1000, Developmental Studies Hybridoma Bank (DSHB), Iowa City, Iowa, USA), mouse anti-HuC/D (16A11, 1:20, Molecular Probes), mouse anti-Neuroilin (zn-8, 1:1000, DSHB), mouse anti-zrf1 (1:400, University of Oregon Monoclonal Antibody Facility), mouse anti-Isl (39.4D5, 1:100, DSHB), rabbit anti-GABA (1:1000, Sigma). For fluorescent detection of antibody labeling, we used Alexa Fluor 568 goat anti-mouse conjugate (1:200, Molecular Probes) and Alexa Fluor 568 goat anti-rabbit conjugate (1:200, Molecular Probes).

In situ RNA hybridization

In situ RNA hybridization was performed as described previously (Hauptmann and Gerster, 2000). Previously described RNA probes included *sox10* (Dutton et al., 2001), *olig2* (Park et al., 2002), *nkx2.2* (Barth and Wilson, 1995), *iro3* (Tan et al., 1999), *shh* (Krauss et al., 1993) and *twhh* (Ekker et al., 1995). Embryos were sectioned as described previously (Park and Appel, 2003). Images were collected using a QImaging Retiga Exi color CCD camera mounted on a compound microscope and imported into Adobe Photoshop. Image manipulations were limited to levels, curves, hue and saturation adjustments.

Cyclopamine treatments

Embryos were incubated in EM containing 100 µM cyclopamine (Toronto Research Chemicals), diluted from a 10 µM stock in ethanol, at 28.5°C. To stop the treatment, embryos were rinsed at least three times in EM.

Morpholino injections

The *twhh* MO, 5'-AAGAGATAATTCAAACGTCATGG-3', has been described previously (Lewis and Eisen, 2001; Nasevicius and Ekker, 2000). Approximately 10 nl of a 1 mg/ml solution was injected into embryos at the one to two-cell stage.

Results

olig2⁺ cells produce motoneurons, interneurons and OPCs

We have previously described transgenic zebrafish in which *olig2* regulatory DNA drives expression of EGFP in a pattern that appears to accurately report transcription of the endogenous *olig2* gene (Shin et al., 2003) (see Fig. S2 in the supplementary material). To more thoroughly characterize *Tg[olig2:egfp]* expression, we labeled embryos with various cell type specific markers. Anti-Isl antibody, which reveals motoneurons in ventral spinal cord, labels a subset of EGFP⁺ cells in 24 hour post fertilization (hpf) embryos (Fig. 1A). Anti-Isl antibody labels both primary motoneurons (PMNs), which begin to be born about 10 hpf, and secondary motoneurons (SMNs), which are born between about 16 and 25 hpf (Myers et al., 1986). In earlier work, we have shown that newly born PMNs express *olig2* at 11.5 hpf (Park et al., 2002). To help discriminate between PMN and SMN populations, we also labeled transgenic embryos with anti-Neuroilin antibody, which reveals SMNs but not PMNs (Fashena and Westerfield, 1999). Doubly labeled cells were evident in transverse sections of 36 hpf embryos (Fig. 1B), showing that *olig2:EGFP⁺* cells give rise to SMNs. In addition, 36 hpf embryos had numerous cells that were *olig2:EGFP⁺*, Neuroilin⁻ (Fig. 1B). Some of these cells might have been neural precursors, as they occupied positions close to the central canal, whereas others were located close to the pial surface of the spinal cord. We confirmed that some *olig2:EGFP⁺* cells were precursors by incubating embryos with BrdU, which marks S-phase cells, from 36 to 48 hpf. Some *olig2:EGFP⁺* cells near the ventricle incorporated BrdU, showing the presence of a proliferative population that is maintained past the period of motoneuron development (Fig. 1C). Notably, only cells that occupied the dorsalmost region of the *olig2:EGFP⁺* domain incorporated BrdU. So that we could compare the distribution of *olig2:EGFP⁺* cells to the pattern of differentiating neurons, we labeled 3 days post fertilization (dpf) transgenic embryos with anti-Hu antibody, which recognizes postmitotic neurons and some S-phase neural cells (Marusich et al., 1994). This revealed ventrally located *olig2:EGFP⁺*, Hu⁺ neurons, *olig2:EGFP⁺*, Hu⁻ cells near the central canal and dorsally and ventrally located *olig2:EGFP⁺*, Hu⁻ cells, which, by their position and multiprocess morphology, were OPCs (Fig. 1D). Some *olig2:EGFP⁺*, Hu⁻ cells had striking radial morphologies. These cells expressed an epitope recognized by zrf-1 antibody (Fig. 1E,F), which labels zebrafish radial glia fibers (Trevarrow et al., 1990). Radial glia produce neurons and astrocytes (Rakic, 2003), raising the possibility that a subset of *olig2:EGFP⁺* cells are maintained as neural precursors into late stages of embryogenesis.

Labeling *Tg[olig2:egfp]* embryos with anti-Hu and anti-Isl antibodies at the same time revealed the presence of EGFP⁺, Hu⁺, Isl⁻ cells (data not shown), suggesting that pMN cells give rise to interneurons as well as motoneurons and OPCs. To test this, we used anti-GABA antibody, which reveals several distinct classes of interneurons in zebrafish embryos (Bernhardt et al., 1992). Transgenic embryos had both EGFP⁺ and EGFP⁻ KA interneurons (Fig. 1G,H,I), which have the distinctive feature that their cell bodies contact the spinal cord

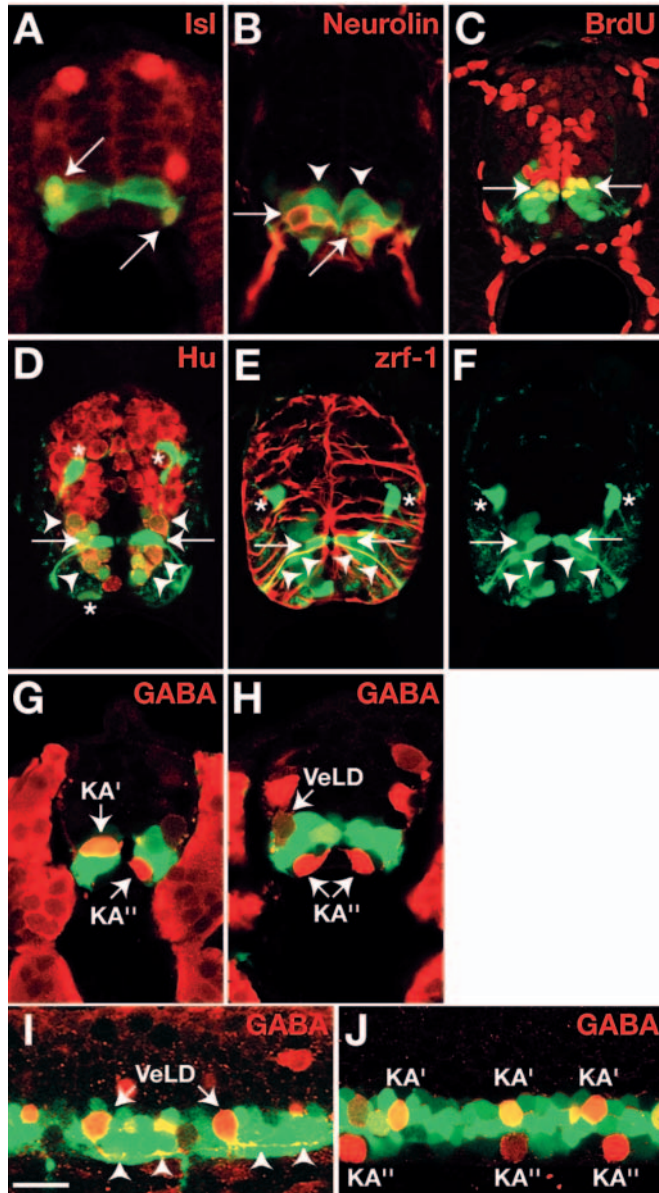


Fig. 1. Spinal cord *olig2*⁺ cells include diverse cell types. (A-H) Transverse sections of *Tg[olig2:egfp]* embryos. Antibodies indicated on each panel. (A) Twenty-four hpf embryo. Arrows indicate *olig2:EGFP*⁺, *Isl*⁺ motoneurons. (B) Thirty-six hpf embryo. Arrows and arrowheads mark *olig2:EGFP*⁺, *Neurolin*⁺ SMNs and *olig2:EGFP*⁺, *Neurolin*⁻ cells, respectively. (C) Forty-eight hpf embryo treated with BrdU from 36 to 48 hpf. Arrows mark *olig2:EGFP*⁺, BrdU⁺ cells (yellow). (D) Three dpf embryo. *olig2:EGFP*⁺ cells include Hu⁺ neurons (arrowheads), dorsally and ventrally migrated Hu⁻ OPCs (asterisks) and Hu⁻ cells with radial morphology (arrows). (E) Three dpf embryo. Arrows and arrowheads mark *olig2:EGFP*⁺, *zrf-1*⁺ radial cells. Asterisks mark dorsally migrated OPCs. (F) EGFP expression, alone, of section shown in E. (G,H) Twenty-four hpf embryo. Anti-GABA labeling reveals *olig2:EGFP*⁺ KA' and putative VeLD interneurons and *olig2:EGFP*⁻ KA'' interneurons. (I,J) Lateral confocal microscope images of 20 hpf (I) and 24 hpf (J) transgenic embryos showing *olig2:EGFP*⁺, GABA⁺ VeLD interneurons, *olig2:EGFP*⁺, GABA⁺ KA' interneurons and *olig2:EGFP*⁻, GABA⁺ KA'' interneurons. Arrowheads in I mark descending axons of VeLD neurons. Scale bar: 20 μ m.

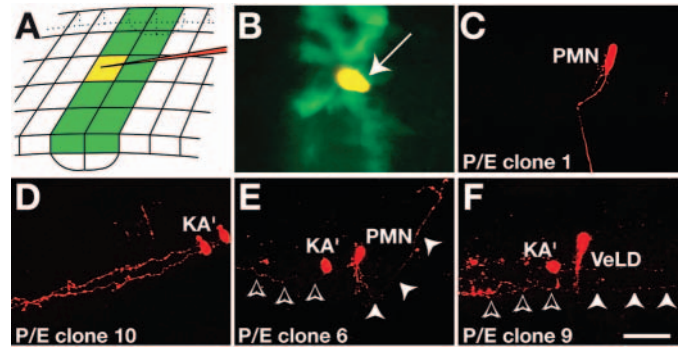


Fig. 2. Clonal analysis of *olig2:EGFP*^{P/E} neural plate cells. (A) Schematic representation of cell labeling strategy. The grid represents cells of the neural plate. Green boxes are *olig2:EGFP*⁺ cells, which, at the time of labeling, overlie the most medial neural plate cells as a consequence of cell movements during early neurulation. (B) Dorsal view of transgenic embryo immediately after labeling. (C-F) Side views, anterior to the left, dorsal up, of 2.5 dpf embryos showing examples of labeled cells, which include PMNs, KA' interneurons and VeLD interneurons. Filled and outlined arrowheads indicate different axon projections. P/E clone numbers correspond to clones in Table 1. Scale bar: 20 μ m for B; 40 μ m for C-F.

central canal. We designated the more dorsal, EGFP⁺ cells as KA' and the more ventral, EGFP⁻ cells as KA''. We also observed GABA⁺ cells near the pial surface that had faint EGFP expression (Fig. 1H). These cells probably were VeLD interneurons (Bernhardt et al., 1990; Bernhardt et al., 1992). We confirmed this by labeling slightly younger embryos, in which EGFP expression was still high in cells that could be distinguished as VeLDs by their axon projections (Fig. 1I). Taken together, these data show that pMN precursors are not limited, in vivo, to producing only motoneurons and OPCs, but that they also give rise to interneurons and radial glia. To more accurately define this precursor population for the following studies, we refer to it hereafter as the *olig2*⁺ precursor population.

Individual *olig2*⁺ cells produce variable, spatially biased lineages

To assess more fully the fates of *olig2*⁺ precursors, we injected individual neural plate cells with vital dye using iontophoresis (Fig. 2A; see Fig. S1 in the supplementary material) and identified clonal descendants by morphology at 2.5 dpf (results summarized in Table 1). We could accurately target individual cells because zebrafish embryos express *olig2* RNA during late gastrulation, prior to neuronal and glial differentiation (Park et al., 2002), and we can see these cells in living *Tg[olig2:egfp]* embryos (Shin et al., 2003). At bud to one-somite stage (10–10.3 hpf), cells that strongly express *olig2:EGFP* lie in an anteroposterior column about two to four cells wide posterior to the position of the first somite (Fig. 2B). These cells overlie *olig2:EGFP*⁻ cells of the most medial region of the neural plate as a result of the morphogenetic cell rearrangements of early neurulation (Schmitz et al., 1993). After neurulation, these cells occupy ventral spinal cord. We refer to this group of medially located cells as the Proximal/Early domain, or *olig2:EGFP*^{P/E}, to reflect the fact that these cells remain proximal to the floor plate as medial becomes ventral during

Table 1. Summary of *olig2*:EGFP^{P/E} clones

P/E clone	PMN	SMN	KA	VeLD	Total
1	1				1
2	1				1
3	1				1
4	1				1
5	1				1
6	1		1		2
7	1		1		2
8	1			1	2
9			1	1	2
10			2		2
11	2		1		3
12	1	2			3
13	2	1			3
14	1	3			4
15	3	1			4
16	2		2		4
17	3		1		4
18	3	2			5

Numbers in first column indicate individual clones arising from *olig2*:EGFP^{P/E} cells of the neural plate. Numbers in remaining columns indicate the number of each type of cell within a clone.

formation of the neural tube. Some injected *olig2*:EGFP^{P/E} cells did not divide and developed as PMNs (Fig. 2C; Table 1), consistent with previous observations that PMNs begin to exit the cell cycle at neural plate stage (Myers et al., 1986). Five labeled cells divided once. In a single instance, the daughter cells were of the same type, with both having ipsilateral axons projecting toward the head, thus identifying them as KA' cells (Fig. 2D). In two cases, the daughters consisted of one PMN and one KA' (Fig. 2E), and in one case one daughter was a PMN and the other a VeLD, identifiable by its ipsilateral descending axon (data not shown). The presence of KA' and VeLD neurons in our clones is consistent with our above observation that *olig2*:EGFP⁺ cells include ventral GABA⁺ cells. The final two-cell clone included a KA' and VeLD (Fig.

2F). Additionally, eight clones had from three to five cells, consisting of either PMNs and KA' cells or PMNs and SMNs (Table 1). Remarkably, no clones contained OPCs.

One possible interpretation of the absence of OPCs from the above clones is that the *olig2*⁺ domain expands with time and, at neural plate stage, *olig2*:EGFP expression does not yet mark precursors that give rise to OPCs. Because it is difficult to label cells after neural plate stage, we instead labeled single *olig2*:EGFP⁻ cells that bordered *olig2*:EGFP^{P/E} cells in the neural plate (Fig. 3A,B). All clonal cells expressed EGFP at 2.5 dpf, although some neurons did so only very weakly (Fig. 3D' and data not shown), suggesting that these cells subsequently downregulated *olig2* expression as shown for motoneurons (Mizuguchi et al., 2001; Novitsch et al., 2001) and VeLD interneurons (Fig. 1). We refer to the origin of these clonal cells as the Distal/Late domain, as the precursor cells, called *olig2*:EGFP^{D/L} cells, are more distal and express EGFP later than *olig2*:EGFP^{P/E} cells. We observed several differences from the *olig2*:EGFP^{P/E} clones. First, clonal sizes were larger, ranging from three to 24 cells, compared with one to five cells for the more proximal clones (Table 2). Second, we observed PMNs only once but all clones contained SMNs (Table 2). Of the 16 clones analyzed, seven consisted of only SMNs (Fig. 3C; Table 2). Third, *olig2*:EGFP^{D/L} cells gave rise to an additional type of interneuron, which had an axon that projected first ventrally and then caudally, and remained ipsilateral. In at least two instances, an ascending axon branched from the main axon (Fig. 3D,F). These cells previously were named CiD (Bernhardt et al., 1990; Hale et al., 2001). Fourth, *olig2*:EGFP^{D/L} cells gave rise to OPCs. These clones never consisted only of OPCs and all lineages that gave rise to OPCs contained SMNs. In two cases, the lineages also contained CiD interneurons (Fig. 3E; Table 2). Similar to the *olig2*:EGFP^{P/E} clones, *olig2*:EGFP^{D/L} clones were variable in cell number and type (Table 2).

In summary, these data show that neural plate cells that contribute to the *olig2*⁺ precursor population are not restricted

Fig. 3. Clonal analysis of *olig2*:EGFP^{D/L} neural plate cells. (A) Schematic representation of labeling strategy. (B) Dorsal view of transgenic embryo immediately after labeling. (C-F) Side views, anterior towards the left, dorsal upwards, of 2.5 dpf embryos showing examples of labeled cells, which include SMNs, CiD interneurons, OPCs (asterisks) and cells whose identities could not be determined (question marks). Arrowheads mark some of the axon projections. (D') Combined images of EGFP and rhodamine fluorescence of clone shown in D. The weak EGFP fluorescence of the CiD interneuron is obscured by the bright rhodamine signal. (D'',F') Schematic of clones shown in D,F. (G) Diagram, from a dorsal view, summarizing fate mapping results showing cell fate bias on the medial/ventral (m/v) to lateral/dorsal (l/d) axis of the neural plate/neural tube. Broken line marks midline of neural plate. Scale bars: 20 μ m.

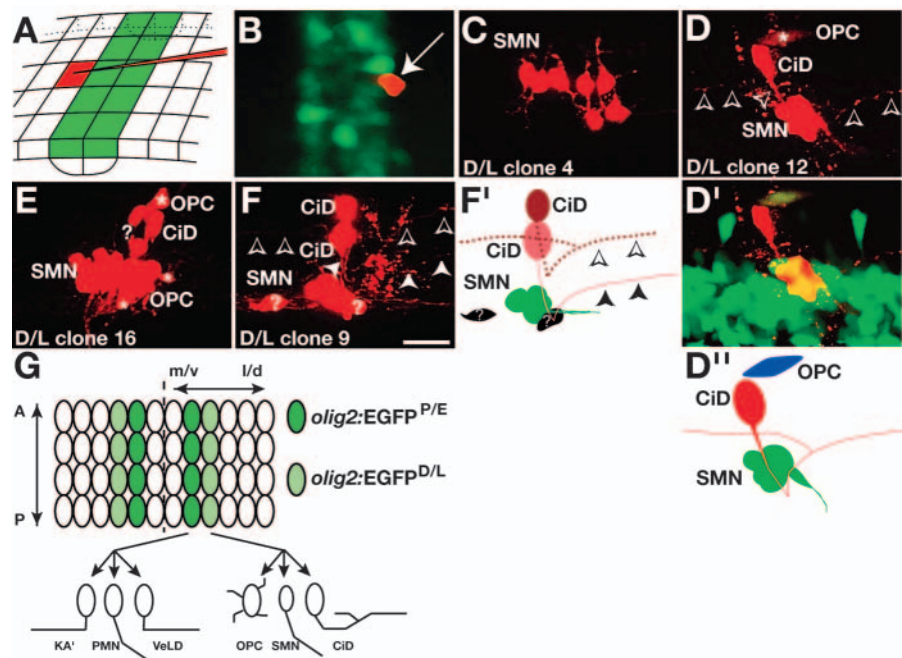


Table 2. Summary of *olig2*:EGFP^{D/L} clones

D/L clone	PMN	SMN	KA	VeLD	CiD	OPC	?	Total
1	3	1	1					5
2		3						3
3		4						4
4		7						7
5		8						8
6		8						8
7		9						9
8		12						12
9		3			2		2	7
10		5	3		3			11
11		4				1		5
12		7			1	1		9
13		12				1		13
14		10				2		12
15		12				3		15
16		18			1	3	2	24

Numbers in first column indicate individual clones arising from cells neighboring *olig2*:EGFP^{D/L} cells of the neural plate. Numbers in remaining columns indicate the number of each type of cell within a clone. Question mark indicates the number of cells that could not be identified.

for either motoneuron or OPC fate and that, surprisingly, they also produce various interneurons. No evidence of consistent lineage patterns exists within our clones. Our results also suggest that the *olig2*⁺ precursor domain expands distally over time and expansion correlates with a spatiotemporal bias in cell fate. In particular, cells that are closest to the midline and express *olig2* early produce mostly PMNs and KA' and VeLD interneurons, and those farther away express *olig2* later and give rise mostly to SMNs, OPCs and CiD interneurons (Fig. 3G).

Motoneurons and OPCs have genetically separable requirements for Hh ligands

The spatial bias evident in our fate-mapping experiments led us to consider if Hh signaling might play a role in specifying different cell fates within the *olig2* precursor domain. Previous work has described three zebrafish *Hh*-related genes and showed that, during early stages of neural development, notochord expresses *shh* and *echidna hedgehog (ehh)*, and floor plate expresses *shh* and *tiggywinkle hedgehog (twhh)* (Currie and Ingham, 1996; Ekker et al., 1995; Krauss et al., 1993). In situ RNA hybridization revealed that at 36 hpf, notochord, medial floor plate and lateral floor plate cells express *shh* (Fig. 4A), whereas only medial floor plate cells express *twhh* (Fig. 4C). Forty-eight hpf embryos express *shh* and *twhh* similar to 36 hpf embryos, except that lateral floor plate cells express little or no *shh* RNA (Fig. 4B,D). Thus, ventral CNS cells of zebrafish embryos express at least two Hh molecules throughout the period of motoneuron and OPC specification.

We next examined neural cell fate in embryos that were deficient for Shh, Twhh or both. First, we reduced Twhh and Shh functions at the same time by injecting *twhh* antisense morpholino oligonucleotides (MO) (Lewis and Eisen, 2001; Nasevicius and Ekker, 2000) into cleavage-stage embryos produced by intercrosses of adults heterozygous for a *syu* mutation, which disrupts the *shh* gene (Schauerte et al., 1998). Injected *syu*^{-/-} embryos, which could be distinguished from wild type by their abnormal body shape, did not express *olig2* and had nearly complete deficits of motoneurons and OPCs

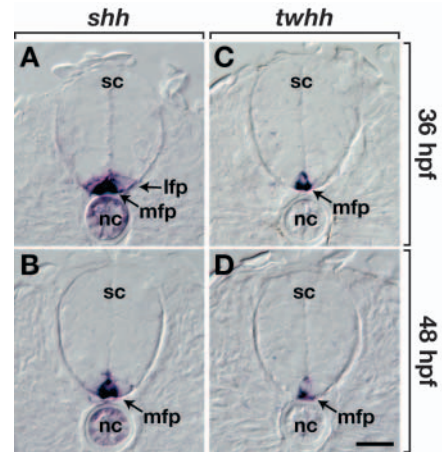


Fig. 4. Zebrafish embryos express Hh ligands during the period of oligodendrocyte specification. All panels show transverse sections through trunk spinal cord (sc), with dorsal upwards. (A) Notochord (nc), medial floor plate (mfp) and lateral floor plate (lfp) express *shh* at 36 hpf. (B) At 48 hpf, medial floor plate and notochord express *shh*. (C) Medial floor plate also expresses *twhh* at 36 hpf and (D) 48 hpf. Scale bar: 20 μ m.

(Fig. 5E-H). This phenotype is similar to that of embryos deficient for Smoothed, a crucial component of the Hh pathway (Chen et al., 2001; Varga et al., 2001), which is necessary for *olig2* expression and OPC development (Park et al., 2002) (data not shown). Next, we found that wild-type embryos injected with *twhh* MO expressed *olig2* and produced motoneurons and OPCs similarly to wild type (Fig. 5I-L). Finally, *olig2*⁺ cells were present in *syu*^{-/-} embryos (Fig. 5M), but they were located more ventrally than normal showing that Shh and Twhh together induce and position the *olig2*⁺ precursor domain. *syu*^{-/-} embryos have normal numbers of PMNs (Lewis and Eisen, 2001), indicating that what we have defined as the *olig2*^{P/E} domain is intact. We also found that these mutant embryos produced SMNs, but in reduced number (Fig. 5N), and they almost entirely lacked OPCs (Fig. 5O,P). Thus, in the absence of Shh function, Twhh induced *olig2* expression, but *olig2*⁺ cells were ectopically positioned and did not give rise to OPCs.

Expansion of the *olig2*⁺ domain is dependent upon Hh signaling and necessary for OPC specification

The absence of OPCs in *syu*^{-/-} embryos could mean that Hh is required to promote expansion of the *olig2*^{P/E} domain to include the *olig2*^{D/L} domain, that Hh is required to specify OPCs from *olig2*⁺ precursors following dorsoventral patterning, or both. We tested these possibilities by using cyclopamine, a specific inhibitor of Smoothed activity (Chen et al., 2002; Incardona et al., 1998) to block the Hh signaling pathway in a time-dependent fashion. To determine the efficacy of cyclopamine as a Hh pathway inhibitor in our experiments, we first incubated embryos continuously in a solution of the drug beginning at 6 hpf, which is prior to initiation of *olig2* expression. These embryos did not express *olig2* and *nkx2.2*, which marks cells in the ventral spinal cord (Barth and Wilson, 1995), at 36 hpf (Fig. 6G,H) and did not develop motoneurons and OPCs by 48 hpf (Fig. 6J,K). Instead, ventral spinal cord cells of these embryos expressed *iro3* (Fig. 6I), which is

normally restricted to dorsal spinal cord cells and a few putative ventral neurons (Tan et al., 1999). Thus, embryos treated at 6 hpf with cyclopamine lacked motoneurons and OPCs because *olig2*⁺ precursors were transformed to a more dorsal fate. This phenotype is consistent with the absence of Shh and Twhh functions, demonstrating that cyclopamine effectively interferes with Hh-mediated spinal cord patterning.

We next tested the possibility that Hh signaling is required continuously for OPC specification by incubating embryos in cyclopamine beginning at 30 hpf, after dorsoventral pattern was established. These embryos did not express *olig2* at 36 hpf (Fig. 6L), showing that Hh signaling is required to maintain *olig2* expression. However, these embryos expressed *nkx2.2* and *iro3* normally (Fig. 6M,N), showing that they otherwise retained appropriate spinal cord dorsoventral patterning. Although these embryos had apparently normal numbers of

motoneurons (Fig. 6O), consistent with the fact that most motoneurons are born prior to 30 hpf (Myers et al., 1986), they did not have OPCs (Fig. 6P,Q). Thus, Hh signaling is required for OPC development subsequent to its role in spinal cord dorsoventral patterning and motoneuron specification.

These data show that Hh signaling is required early to initiate the dorsoventral patterning process that forms the *olig2*⁺ precursor domain and late to drive *olig2* precursors into an oligodendrocyte pathway. To test the idea that Hh signaling also regulates spatiotemporally biased fate specification within the *olig2*⁺ precursor domain, we next performed a series of cyclopamine addition and washout experiments. First, we incubated embryos in cyclopamine from 6–26 hpf. When examined at 26 hpf, these embryos did not express *olig2* (Fig. 7A) but, instead, expressed *iro3* throughout the spinal cord (Fig. 7B, compare with normal pattern in Fig. 6C). These

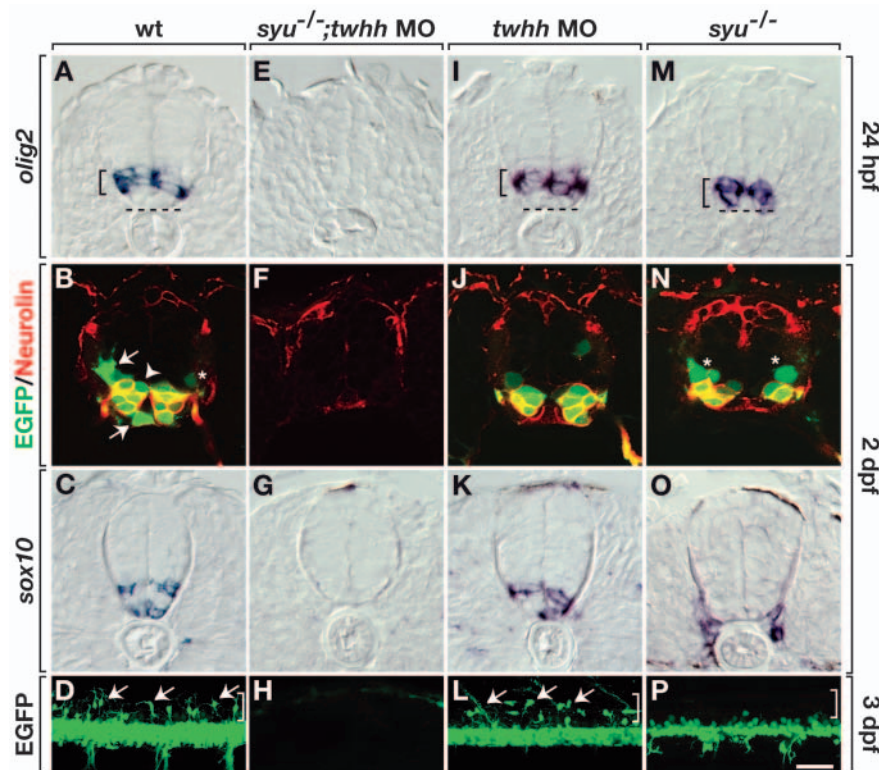


Fig. 5. Motoneurons and oligodendrocytes have genetically separable requirements for Hh signaling. Top three rows of panels show transverse sections through trunk spinal cord, with dorsal upwards. Bottom row shows lateral views of intact *olig2:egfp* embryos, with dorsal upwards and anterior towards the left. (A) Wild-type embryos expressed *olig2* RNA in the ventral spinal cord (bracket), but the ventralmost cells were *olig2*⁻. Broken line indicates the ventral boundary of the spinal cord. (B) *olig2:EGFP*⁺ cells of wild-type embryos included Neuroilin⁺ SMNs, OPCs (arrows), Neuroilin⁻ cells near ventricle (arrowhead) and a faint GFP⁺, Neuroilin⁻ cell near pial surface (asterisk), which could be a primary motoneuron or VeLD interneuron. (C) *sox10*⁺ OPCs in wild-type embryo. (D) Arrows indicate dorsally migrated OPCs in wild-type embryo. Bracket indicates dorsal spinal cord. (E–H) *syu*^{-/-} embryos injected with *twhh* MO lacked *olig2*⁺ cells (E), secondary motoneurons (F) and OPCs (G,H). (I–L) Wild-type embryos injected with *twhh* MO expressed *olig2* RNA (I) and produced secondary motoneurons (J) and OPCs (K,L). *syu*^{-/-} embryos expressed *olig2* RNA (M), but *olig2*⁺ cells were located more ventrally than normal. (M–P) *syu*^{-/-} embryos had *olig2:EGFP*⁺, Neuroilin⁺ secondary motoneurons and *olig2:EGFP*⁺, Neuroilin⁻ cells (asterisks) (N); however, they did not have OPCs (O,P). (O) *sox10*⁺ cells are probably Schwann cells (Dutton et al., 2001), which do not appear in all sections. Scale bar: 20 μm for upper three rows; 40 μm for bottom row.

embryos also did not express *olig2* (Fig. 7C) or *sox10* (Fig. 7D) at 36 hpf and 48 hpf, respectively. Thus, release of Smoothed inhibition after dorsoventral spinal cord pattern was established was not sufficient to recover *olig2*⁺ precursors or OPCs. Next, we incubated embryos in cyclopamine from 11–26 hpf. These embryos also did not express *olig2* at 26 hpf (Fig. 7E), however, the ventral most spinal cord cells did not express *iro3* (Fig. 7F), showing that dorsoventral spinal cord patterning was at least partially intact. In contrast to 6–26 hpf-treated embryos, by 36 hpf ventral spinal cord cells of 11–26 hpf-treated embryos expressed *olig2* (Fig. 7G). Thus, in the absence of Hh signaling during this period, embryos maintained a population of spinal cord cells that were competent to express *olig2* once they were removed from cyclopamine. A notable difference to untreated embryos is that *olig2* was expressed by the ventral-most spinal cord cells of 11–26 hpf treated embryos (compare with Fig. 6A). One explanation is that Hh signaling is continually required to maintain ventral spinal cord precursor domains. Therefore, if Hh signaling is blocked soon after initiation of the dorsoventral patterning process, precursor domains shift ventralwards. Despite the fact that these embryos expressed *olig2*, they had few OPCs (Fig. 7H; Fig. 8C,D,G) and reduced number of SMNs (Fig. 8G).

We reasoned that the absence of OPCs in the above experiments might have resulted from failure to form the *olig2*^{D/L} precursor population, which is the origin of OPCs. To test this, we added cyclopamine at 14 hpf rather than 11 hpf. As before, these embryos did not express *olig2* at 26 hpf (Fig. 7I). Labeling with *iro3* probe revealed an *iro3*⁻ domain that was enlarged dorsally (Fig. 7J) compared with embryos treated starting at 11 hpf (Fig. 7F). At 36 hpf,

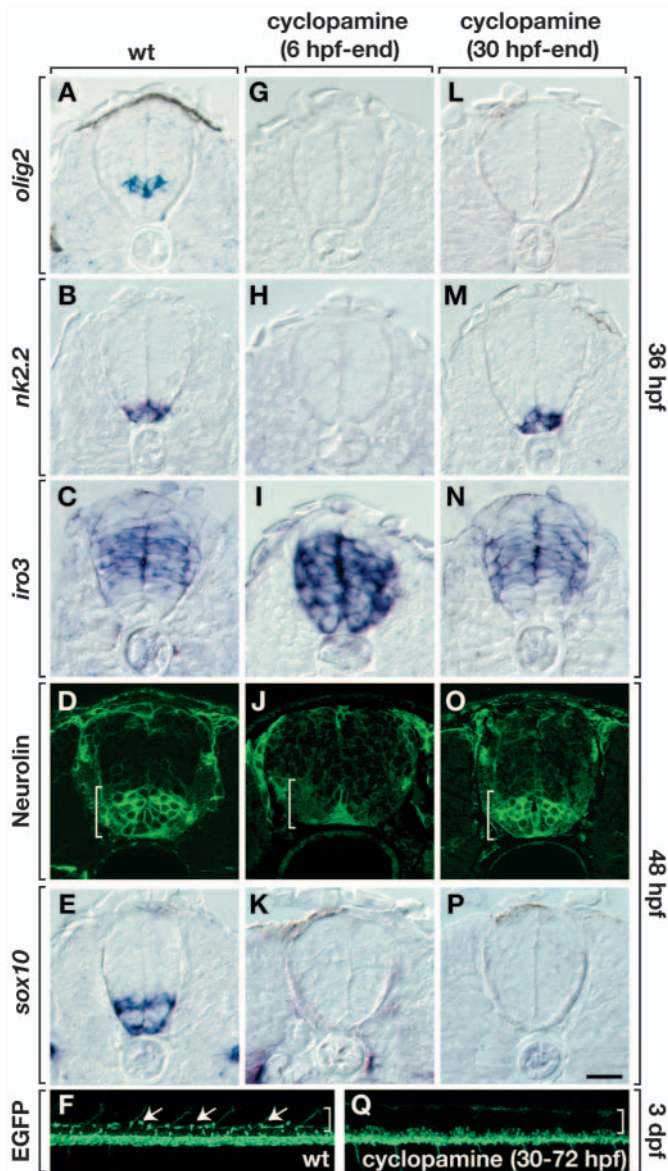


Fig. 6. Hh signaling is required for oligodendrocyte specification after dorsoventral spinal cord patterning and motoneuron development. All panels in the top five rows show transverse sections, dorsal upwards, of trunk spinal cord. Bottom two panels are side views of whole embryos, dorsal upwards and anterior leftwards. (A-E) Control embryos showing normal expression of various markers. (G-K) Embryos treated with cyclopamine from 6 hpf onwards did not express *olig2* (G) or *nkx2.2* (H), and expressed *iro3* in ventral spinal cord (I), indicating that ventral spinal cord patterning was lost. These embryos did not produce SMNs (J) or OPCs (K). (L-Q) Embryos treated with cyclopamine from 30 hpf onward did not express *olig2* by 36 hpf (L) but expressed *nkx2.2* (M) and *iro3* (N) in their normal patterns. SMNs were produced in normal numbers (O) but OPCs were absent (P,Q). (F) Untreated *Tg[olig2:egfp]* embryo showing OPCs (arrows) in dorsal spinal cord (brackets). Scale bar: 20 μ m for top five rows; 80 μ m for F and Q.

ventral spinal cord cells of these embryos expressed *olig2* (Fig. 7K) and the *olig2*⁺ domain was dorsally expanded compared with embryos treated at 11 hpf (Fig. 7G). Again, *olig2*⁺ cells were more ventral than normal, in contrast to those treated at

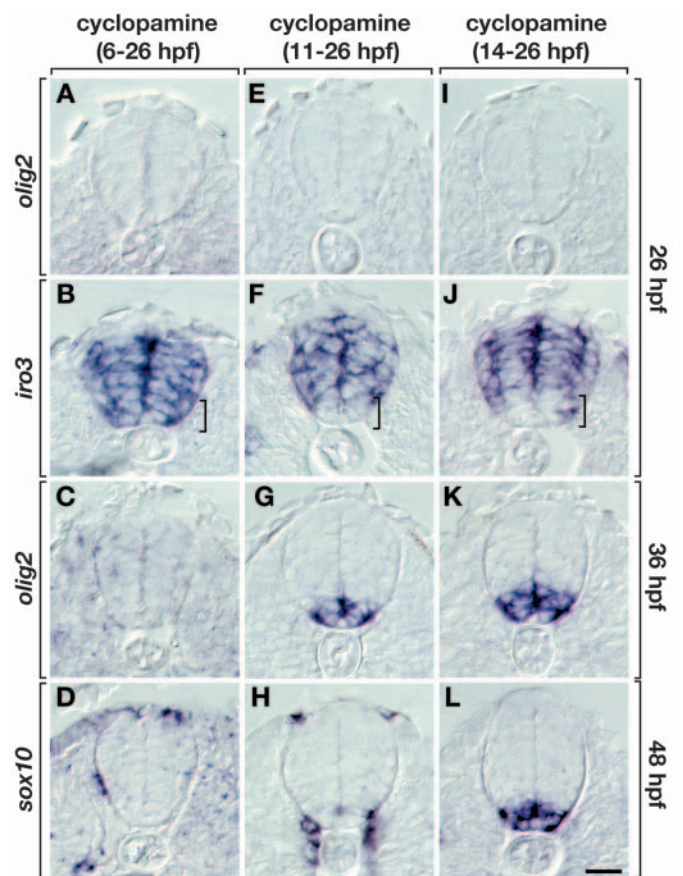


Fig. 7. Conditional manipulation of Hh signaling reveals a crucial period for specification of oligodendrocyte precursors. All panels show transverse sections, dorsal side upwards. (A-D) Embryos incubated in cyclopamine from 6–26 hpf. At 26 hpf, these embryos did not express *olig2* (A). *iro3* expression included the ventralmost spinal cord cells (B; brackets in B,F,J). *olig2* expression was not recovered by 36 hpf (C) and no *sox10*⁺ OPCs were evident by 48 hpf (D). (E–H) Embryos treated with cyclopamine from 11–26 hpf. *olig2* expression was absent by 26 hpf (E) but a small domain of *iro3*⁺ cells was present in the ventral spinal cord (F). These embryos recovered *olig2* expression by 36 hpf, but in an abnormally ventral position (G). At 48 hpf, few *sox10*⁺ OPCs had developed (H). (I–L) Embryos treated with cyclopamine from 14–26 hpf. *olig2* expression was not maintained until 26 hpf (I) but *iro3* expression appeared normal (J, compare with Fig. 6C). *olig2* expression was recovered by 36 hpf in ventralmost spinal cord cells (K) but in a larger domain compared with 11–26 hpf treated embryos. These embryos expressed *sox10* at 48 hpf, but in an abnormally ventral position (L, compare with Fig. 6E). Scale bar: 20 μ m.

11 hpf, these embryos expressed *sox10* (Fig. 7L). Consistent with the ventralward shift of *olig2* expression, *sox10*⁺ cells were more ventral than normal. They also appeared to be more numerous (compare with Fig. 5C).

Modulation of Hh signaling can shift the balance between motoneuron and OPC production

To explain the apparent increase in *sox10*⁺ OPCs, we considered the possibility that blocking Hh signaling during 14–26 hpf shifts *olig2*^{D/L} precursors from SMN to OPC fate, as this period coincides with the birth of most SMNs. To

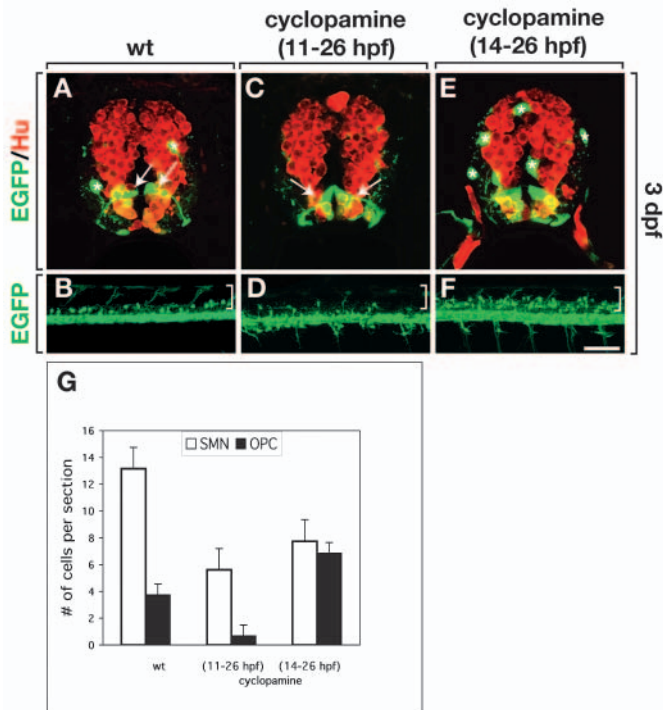


Fig. 8. Modulation of Hh signaling can promote OPC specification at the expense of secondary motoneurons. (A,C,E) Transverse sections, dorsal upwards, of *Tg[olig2:egfp]* embryos labeled with pan-neuronal anti-Hu antibody (red). Asterisks and arrows mark OPCs and radial cells, respectively. (B,D,F) Lateral views of intact *Tg[olig2:egfp]* embryos, dorsal upwards and anterior leftwards. Brackets indicate dorsal spinal cord. (A,B) Untreated embryos showing normal number and distribution of OPCs. (C,D) Embryos treated with cyclopamine from 11-26 hpf had few OPCs. (E,F) Embryos treated from 14-26 hpf had excess OPCs. (G) Quantification of effects on SMNs and OPCs. Embryos were labeled with anti-Neurolin antibody to reveal SMNs. A total of 20 sections were counted from four embryos for each experiment. Scale bar: 20 μ m for top row; 80 μ m for bottom row.

investigate this, we repeated the cyclopamine treatments on *Tg[olig2:egfp]* embryos and compared OPC and motoneuron development. Compared with wild-type controls (Fig. 8A,B,G), embryos treated from 11-26 hpf had a severe deficit of OPCs (Fig. 8C,D,G) and fewer SMNs (Fig. 8C,G), although the general pattern of neurogenesis, revealed by expression of the pan-neuronal marker, Hu, appeared normal (Fig. 8C). By contrast, embryos treated from 14-26 hpf had a 1.8-fold excess of OPCs and a 1.7-fold decrease in secondary motoneurons compared with wild type (Fig. 8E-G). The complementary increase and decrease in these cell types strongly suggests that a temporary block of Hh signaling can redirect precursors that would normally develop as SMNs for OPC fate.

Discussion

Cell fate specification within the *olig2*⁺ precursor domain is spatially and temporally regulated

A predominant model of fate specification for the spinal cord is that distinct precursor domains first produce a particular type of neuron (Jessell, 2000; Lee and Pfaff, 2001) and then either

oligodendrocytes or astrocytes (Anderson, 2001; Rowitch, 2004). However, results of cell lineage analyses in chick and zebrafish embryos suggest that spinal cord precursors give rise to a greater variety of cell types than gene expression patterns reveal (Leber et al., 1990; Papan and Campos-Ortega, 1997; Papan and Campos-Ortega, 1999). To bridge the gap between lineage analyses, which were performed in the absence of knowledge of specific spinal cord precursor domains, and gene expression studies, we investigated the fate of individual neural plate cells that express *olig2:EGFP*. Our observations reveal several key new insights to the problem of cell fate specification within this ventral spinal cord precursor domain. First, in addition to motoneurons and OPCs, *olig2:EGFP*⁺ precursors gave rise to at least three distinct interneurons in zebrafish. This rules out the simple idea that a binary fate decision specifies *olig2*⁺ precursors for either motoneuron or OPC fate. Second, consistent patterns of progeny cells were not evident among the clones. This fits best with the possibility that cell fate is influenced by extrinsically acting factors that vary in space and time, as proposed for retina (Livesey and Cepko, 2001), rather than by inheritance of factors that specify formation of particular lineages that arise repeatedly within ventral spinal cord. Third, clones frequently consisted of mixed cell types. This was particularly true of *olig2:EGFP*^{P/E} neural plate clones in which almost every labeled cell that divided produced two different kinds of neurons. This is similar to the pattern of cell types produced by ganglion mother cells in flies and raises the possibility that asymmetric distribution of factors such as Numb contributes to diversification of neurons in ventral spinal cord. Fourth, motoneurons, OPCs and even interneurons arose within the same clones marked at neural plate stage. Thus, individual cells that expressed *olig2:EGFP* were not restricted for motoneuron or OPC fate. Although we do not know when motoneurons and OPCs segregate within lineages, our data show that lineages have not diverged at early stages of neurogenesis, favoring a 'switching' model over a 'segregating' model (Rowitch et al., 2002). Finally, *olig2:EGFP*⁺ expression does not mark a homogeneous population of spinal cord precursors. Instead, both the proliferative potential and developmental fate of *olig2:EGFP*⁺ precursors are spatiotemporally biased, revealing a more finely graded patterning system than previously appreciated.

Spatial and temporal roles for Hh signaling in patterning the *olig2*⁺ precursor domain

An obvious candidate for regulating formation and patterning of the *olig2*⁺ precursor domain is the Hh signaling system. The idea that a morphogenetic gradient of Shh establishes distinct precursor domains in the ventral spinal cord is well established (Jessell, 2000; Lee and Pfaff, 2001). However, whether Hh signaling also regulates fate specification within a precursor domain has not been explored. Our work now shows that Hh signaling is necessary at multiple steps during neural development to specify oligodendrocytes from precursors that also produce motoneurons and interneurons (Fig. 9).

The first step at which Hh signaling acts is to induce and position the *olig2*⁺ precursor domain in the developing spinal cord. Spinal cord cells did not express *olig2*⁺ and, consequently, did not produce motoneurons and oligodendrocytes in zebrafish embryos that were deficient for both Shh and Twhh. By contrast, *olig2*⁺ cells were present in

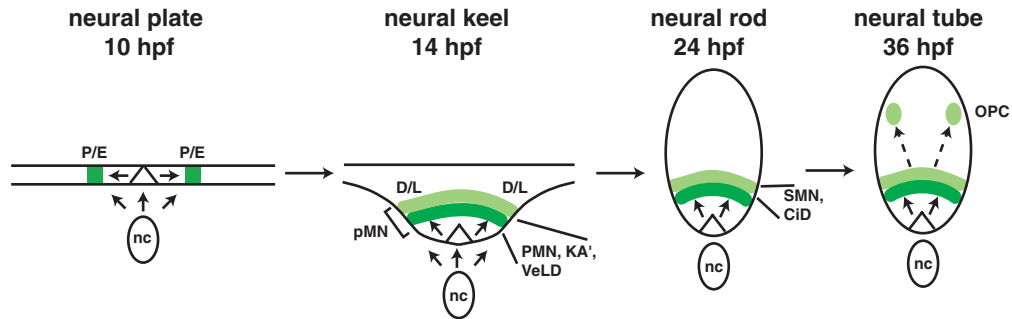


Fig. 9. Summary of Hh signaling and ventral spinal cord patterning in zebrafish. Arrows represent Hh ligands expressed by notochord (nc) and floor plate (triangle). The *olig2*^{P/E} domain (dark green) is formed at neural plate stage and expands to include the *olig2*^{D/L} domain (light green) by neural keel stage. Together, these comprise the pMN precursor domain. We propose that PMNs, KAs and VeLDs are produced first, from *olig2*^{P/E}, followed by SMNs and CiDs and, later, OPCs from *olig2*^{D/L}. Broken lines represent OPC dorsal migration.

embryos deficient only for Shh, but shifted ventrally compared with wild type. Thus, Twhh can induce *olig2* expression, but only in cells located close to the source of Twhh. These observations suggest that, in zebrafish, Shh and Twhh form a combined gradient of Hh signaling activity to properly specify and position the *olig2*⁺ precursor domain.

Once Hh signaling induces *olig2* expression within a subset of spinal cord precursors, it is required continuously during early stages of neurogenesis to maintain its expression. We showed that embryos treated with cyclopamine at 11 or 14 hpf, after initiation of *olig2* transcription, no longer expressed *olig2* by 26 hpf. However, if they were then removed from the cyclopamine, by 36 hpf they re-expressed *olig2*, but in a domain ventral to the normal position of *olig2*⁺ cells. These *in vivo* results are similar to work that showed that ventral neural plate explants cultured in the absence of Shh re-expressed Pax7, a marker of dorsal spinal cord, whereas slightly older ventral neural explants did not (Ericson et al., 1996). Together, these data suggest that during early stages of neural development, neural cells are plastic and require an extended period of exposure to Hh signals to stabilize ventral precursor domains.

We also found that the entire *olig2*⁺ precursor domain appears to be formed dynamically by continuous exposure to Hh signals rather than all at once (Fig. 9). Our fate mapping showed that *olig2*:EGFP⁻ cells that border *olig2*:EGFP⁺ cells in the neural plate in wild-type embryos at 10 hpf later express the transgene and it is specifically these cells that produce many of the secondary motoneurons and all of the OPCs. Our functional data suggest that Hh signaling promotes expansion of the *olig2*⁺ domain and OPC production. First, *syu*^{-/-} embryos express *olig2* but they have fewer than normal secondary motoneurons and almost no OPCs. *syu*^{-/-} embryos were previously shown to have appropriate numbers of primary motoneurons (Lewis and Eisen, 2001), which we show originate within the *olig2*^{P/E} domain. One possible interpretation of these observations is that Shh is required for formation of the *olig2*^{D/L} domain but not the *olig2*^{P/E} domain. Second, embryos treated with cyclopamine from 14–26 hpf had dorsally enlarged *olig2*⁺ domains relative to those treated from 11–26 hpf and only the 14–26 hpf group produced OPCs. We interpret our data to mean that, in zebrafish, exposure to Hh between 11 and 14 hpf is crucial for expanding the *olig2*^{P/E} domain to include the *olig2*^{D/L} domain, which gives rise to OPCs. We conclude that although all pMN precursors express

olig2, they do so at different times and that this correlates with a spatial bias in cell fate. Thus, time and position dependent specification of *olig2*⁺ precursors by Hh signaling contributes to cell fate diversification (Fig. 9).

Subsequent to formation of the *olig2*⁺ domain, a differential response of *olig2*^{D/L} cells to Hh signals apparently determines whether they develop as SMNs or OPCs. In particular, if we blocked Hh signaling with cyclopamine from 14 hpf–26 hpf, during the period of SMN birth, we later found that these embryos had deficits of SMNs, suggesting that continuous exposure to hedgehog proteins is necessary to drive an *olig2*⁺ cell into that differentiation pathway. Similarly, by applying recombinant Shh and function-blocking anti-Shh antibodies to neural explants, Ericson et al. (Ericson et al., 1996) produced evidence interpreted to mean that Shh first ventralizes the spinal cord and then later (until late S-phase prior to cell cycle exit) promotes motoneuron development from ventralized precursors. However, these experiments did not establish the fate of ventralized precursors from which Shh was then removed by function-blocking antibody. Our cyclopamine data show that secondary motoneuron deficits were accompanied by complementary increases in OPC number, if Hh signaling was restored after the period of motoneuron development. Thus, differential response of *olig2*⁺ precursors to Hh signals could specify them as motoneurons or OPCs. Recent work described methods to promote formation of motoneurons from embryonic stem cells in culture (Wichterle et al., 2002). Our results raise the possibility that modulation of Hh signaling could enrich the production of oligodendrocytes from the same cultures.

Finally, our data provide strong evidence that Hh signaling is required for OPC specification in a manner independent from its role in spinal cord dorsoventral patterning. Similar to function blocking anti-Shh antibody experiments (Orentas et al., 1999; Soula et al., 2001), our cyclopamine experiments showed that Hh signaling is necessary until the time that OPCs normally appear, well after dorsoventral patterning is completed. These data favor the idea that late Hh signaling plays a direct role in OPC specification rather than an indirect one, through induction of a secondary signaling pathway. As this late requirement is similar to a late requirement for Hh signaling in motoneuron specification (Ericson et al., 1996), our results raise the possibility that Hh acts as a general signal to drive *olig2*⁺ cells into a differentiation pathway.

Recently reported work has provided evidence that the timing of Hh signaling plays an important part in specifying distinct muscle cells in zebrafish (Wolff et al., 2003). Similarly, different responses to Hh over time appear to contribute to patterning of the telencephalon (Kohtz et al., 1998). Our own studies now show that the variety of cell types that arise from a common ventral spinal cord precursor population is rich and modulation of Hh signaling can influence the kinds of cells that this population produces. Thus, Hh not only functions as a morphogen to establish a precursor domain, but also subsequently contributes to diversification of cell fate within it.

We gratefully acknowledge the contributions of the following individuals: Judith Eisen and Kate Lewis for *twhh* morpholino; Lee Dixon and Laura McClung for technical help; and Lila Solnica-Krezel and Michael Cooper for comments on the manuscript. The anti-BrdU, anti-Isl and anti-Neuroilin antibodies, developed by S. J. Kaufman, T. M. Jessell and B. Trevarrow, respectively, were obtained from the Developmental Studies Hybridoma Bank developed under the auspices of the NICHD and maintained by The University of Iowa, Department of Biological Sciences, Iowa City, IA 52242. Confocal microscopy was performed using equipment made available by the VUMC Cell Imaging Core Resource, supported by NIH grants 1S10RR15682-1, CA68485 and DK20593. Funds for this work were provided by the National Multiple Sclerosis Society and NIH grants HD3118 and NS46668.

Supplementary material

Supplementary material for this article is available at <http://dev.biologists.org/cgi/content/full/131/23/5959/DC1>

References

- Anderson, D. J. (2001). Stem cells and pattern formation in the nervous system: the possible versus the actual. *Neuron* **30**, 19-35.
- Barresi, M. J., Stickney, H. L. and Devoto, S. H. (2000). The zebrafish slow-muscle-omitted gene product is required for Hedgehog signal transduction and the development of slow muscle identity. *Development* **127**, 2189-2199.
- Barth, K. A. and Wilson, S. W. (1995). Expression of zebrafish nk2.2 is influenced by sonic hedgehog/vertebrate hedgehog-1 and demarcates a zone of neuronal differentiation in the embryonic forebrain. *Development* **121**, 1755-1768.
- Bernhardt, R. R., Chitnis, A. B., Lindamer, L. and Kuwada, J. Y. (1990). Identification of spinal neurons in the embryonic and larval zebrafish. *J. Comp. Neurol.* **302**, 603-616.
- Bernhardt, R. R., Patel, C. K., Wilson, S. W. and Kuwada, J. Y. (1992). Axonal trajectories and distribution of GABAergic spinal neurons in wildtype and mutant zebrafish lacking floor plate cells. *J. Comp. Neurol.* **326**, 263-272.
- Chen, J. K., Taipale, J., Cooper, M. K. and Beachy, P. A. (2002). Inhibition of Hedgehog signaling by direct binding of cyclopamine to Smoothened. *Genes Dev.* **16**, 2743-2748.
- Chen, W., Burgess, S. and Hopkins, N. (2001). Analysis of the zebrafish smoothened mutant reveals conserved and divergent functions of hedgehog activity. *Development* **128**, 2385-2396.
- Currie, P. D. and Ingham, P. W. (1996). Induction of a specific muscle cell type by a hedgehog-like protein in zebrafish. *Nature* **382**, 452-455.
- Dutton, K. A., Pauliny, A., Lopes, S. S., Elworthy, S., Carney, T. J., Rauch, J., Geisler, R., Haffter, P. and Kelsh, R. N. (2001). Zebrafish colourless encodes *sox10* and specifies non-ectomesenchymal neural crest fates. *Development* **128**, 4113-4125.
- Eisen, J. S., Pike, S. H. and Debu, B. (1989). The growth cones of identified motoneurons in embryonic zebrafish select appropriate pathways in the absence of specific cellular interactions. *Neuron* **2**, 1097-1104.
- Ekker, S. C., Ungar, A. R., Greenstein, P., von Kessler, D. P., Porter, J. A., Moon, R. T. and Beachy, P. A. (1995). Patterning activities of vertebrate hedgehog proteins in the developing eye and brain. *Curr. Biol.* **5**, 944-955.
- Ericson, J., Morton, S., Kawakami, A., Roelink, H. and Jessell, T. M. (1996). Two critical periods of Sonic Hedgehog signaling required for the specification of motor neuron identity. *Cell* **87**, 661-673.
- Fashena, D. and Westerfield, M. (1999). Secondary motoneuron axons localize DM-GRASP on their fasciculated segments. *J. Comp. Neurol.* **406**, 415-424.
- Hale, M. E., Ritter, D. A. and Fetcho, J. R. (2001). A confocal study of spinal interneurons in living larval zebrafish. *J. Comp. Neurol.* **437**, 1-16.
- Hauptmann, G. and Gerster, T. (2000). Multicolor whole-mount in situ hybridization. *Methods Mol. Biol.* **137**, 139-148.
- Incardona, J. P., Gaffield, W., Kapur, R. P. and Roelink, H. (1998). The teratogenic Veratrum alkaloid cyclopamine inhibits sonic hedgehog signal transduction. *Development* **125**, 3553-3562.
- Jessell, T. M. (2000). Neuronal specification in the spinal cord: inductive signals and transcriptional codes. *Nat. Rev. Genet.* **1**, 20-29.
- Kimmel, C. B., Ballard, W. W., Kimmel, S. R., Ullmann, B. and Schilling, T. F. (1995). Stages of embryonic development of the zebrafish. *Dev. Dyn.* **203**, 253-310.
- Kohtz, J. D., Baker, D. P., Corte, G. and Fishell, G. (1998). Regionalization within the mammalian telencephalon is mediated by changes in responsiveness to Sonic Hedgehog. *Development* **125**, 5079-5089.
- Krauss, S., Concordet, J. P. and Ingham, P. W. (1993). A functionally conserved homolog of the Drosophila segment polarity gene *hh* is expressed in tissues with polarizing activity in zebrafish embryos. *Cell* **75**, 1431-1444.
- Leber, S. M., Breedlove, S. M. and Sanes, J. R. (1990). Lineage, arrangement, and death of clonally related motoneurons in chick spinal cord. *J. Neurosci.* **10**, 2451-2462.
- Lee, S. K. and Pfaff, S. L. (2001). Transcriptional networks regulating neuronal identity in the developing spinal cord. *Nat. Neurosci. Suppl.* **4**, 1183-1191.
- Lewis, K. E. and Eisen, J. S. (2001). Hedgehog signaling is required for primary motoneuron induction in zebrafish. *Development* **128**, 3485-3495.
- Livesey, F. J. and Cepko, C. L. (2001). Vertebrate neural cell-fate determination: lessons from the retina. *Nat. Rev. Neurosci.* **2**, 109-118.
- Lu, Q. R., Sun, T., Zhu, Z., Ma, N., Garcia, M., Stiles, C. D. and Rowitch, D. H. (2002). Common developmental requirement for Olig function indicates a motor neuron/oligodendrocyte connection. *Cell* **109**, 75-86.
- Lu, Q. R., Yuk, D., Alberta, J. A., Zhu, Z., Pawlitzky, I., Chan, J., McMahon, A. P., Stiles, C. D. and Rowitch, D. H. (2000). Sonic hedgehog-regulated oligodendrocyte lineage genes encoding bHLH proteins in the mammalian central nervous system. *Neuron* **25**, 317-329.
- Marusich, M. F., Furneaux, H. M., Henion, P. D. and Weston, J. A. (1994). Hu neuronal proteins are expressed in proliferating neurogenic cells. *J. Neurobiol.* **25**, 143-155.
- Mizuguchi, R., Sugimori, M., Takebayashi, H., Kosako, H., Nagao, M., Yoshida, S., Nabeshima, Y., Shimamura, K. and Nakafuku, M. (2001). Combinatorial roles of *olig2* and *neurogenin2* in the coordinated induction of pan-neuronal and subtype-specific properties of motoneurons. *Neuron* **31**, 757-771.
- Myers, P. Z., Eisen, J. S. and Westerfield, M. (1986). Development and axonal outgrowth of identified motoneurons in the zebrafish. *J. Neurosci.* **6**, 2278-2289.
- Nasevicius, A. and Ekker, S. C. (2000). Effective targeted gene 'knockdown' in zebrafish. *Nat. Genet.* **26**, 216-220.
- Novitsch, B. G., Chen, A. I. and Jessell, T. M. (2001). Coordinate regulation of motor neuron subtype identity and pan-neuronal properties by the bHLH repressor *Olig2*. *Neuron* **31**, 773-789.
- Orentas, D. M., Hayes, J. E., Dyer, K. L. and Miller, R. H. (1999). Sonic hedgehog signaling is required during the appearance of spinal cord oligodendrocyte precursors. *Development* **126**, 2419-2429.
- Papan, C. and Campos-Ortega, J. A. (1997). A clonal analysis of spinal cord development in the zebrafish. *Dev. Genes. Evol.* **207**, 71-81.
- Papan, C. and Campos-Ortega, J. A. (1999). Region-specific cell clones in the developing spinal cord of the zebrafish. *Dev. Genes. Evol.* **209**, 135-144.
- Park, H., Mehta, A., Richardson, J. S. and Appel, B. (2002). *olig2* is required for zebrafish primary motor neuron and oligodendrocyte development. *Dev. Biol.* **248**, 356-368.
- Park, H.-C. and Appel, B. (2003). Delta-Notch signaling regulates oligodendrocyte specification. *Development* **130**, 3747-3755.
- Poh, A., Karunaratne, A., Kolle, G., Huang, N., Smith, E., Starkey, J., Wen, D., Wilson, I., Yamada, T. and Hargrave, M. (2002). Patterning of the vertebrate ventral spinal cord. *Int. J. Dev. Biol.* **46**, 597-608.
- Pringle, N. P., Yu, W. P., Howell, M., Colvin, J. S., Ornitz, D. M. and Richardson, W. D. (2003). Fgfr3 expression by astrocytes and their

- precursors: evidence that astrocytes and oligodendrocytes originate in distinct neuroepithelial domains. *Development* **130**, 93-102.
- Rakic, P.** (2003). Elusive radial glial cells: historical and evolutionary perspective. *Glia* **43**, 19-32.
- Richardson, W. D., Smith, H. K., Sun, T., Pringle, N. P., Hall, A. and Woodruff, R.** (2000). Oligodendrocyte lineage and the motor neuron connection. *Glia* **29**, 136-142.
- Rowitch, D. H.** (2004). Glial specification in the vertebrate neural tube. *Nat. Rev. Neurosci.* **5**, 409-419.
- Rowitch, D. H., Lu, Q. R., Kessaris, N. and Richardson, W. D.** (2002). An 'oligarchy' rules neural development. *Trends Neurosci.* **25**, 417-422.
- Schauerte, H. E., van Eeden, F. J., Fricke, C., Odenthal, J., Strahle, U. and Haffter, P.** (1998). Sonic hedgehog is not required for the induction of medial floor plate cells in the zebrafish. *Development* **125**, 2983-2993.
- Schmitz, B., Papan, C. and Campos-Ortega, J. A.** (1993). Neurulation in the anterior trunk region of the zebrafish *Brachydanio rerio*. *Roux's Arch. Dev. Biol.* **202**, 250-259.
- Shin, J., Park, H.-C., Topczewska, J. M., Mawdsley, D. J. and Appel, B.** (2003). Neural cell fate analysis in zebrafish using olig2 BAC transgenics. *Methods Cell Sci.* **25**, 7-14.
- Shirasaki, R. and Pfaff, S. L.** (2002). Transcriptional codes and the control of neuronal identity. *Annu. Rev. Neurosci.* **25**, 251-281.
- Soula, C., Danesin, C., Kan, P., Grob, M., Poncet, C. and Cochard, P.** (2001). Distinct sites of origin of oligodendrocytes and somatic motoneurons in the chick spinal cord: oligodendrocytes arise from Nkx2.2-expressing progenitors by a Shh-dependent mechanism. *Development* **128**, 1369-1379.
- Stolt, C. C., Lommes, P., Sock, E., Chaboissier, M. C., Schedl, A. and Wegner, M.** (2003). The Sox9 transcription factor determines glial fate choice in the developing spinal cord. *Genes Dev.* **17**, 1677-1689.
- Takebayashi, H., Nabeshima, Y., Yoshida, S., Chisaka, O. and Ikenaka, K.** (2002). The basic helix-loop-helix factor olig2 is essential for the development of motoneuron and oligodendrocyte lineages. *Curr. Biol.* **12**, 1157-1163.
- Takebayashi, H., Yoshida, S., Sugimori, M., Kosako, H., Kominami, R., Nakafuku, M. and Nabeshima, Y.** (2000). Dynamic expression of basic helix-loop-helix Olig family members: implication of Olig2 in neuron and oligodendrocyte differentiation and identification of a new member, Olig3. *Mech. Dev.* **99**, 143-148.
- Tan, J. T., Korzh, V. and Gong, Z.** (1999). Expression of a zebrafish iroquois homeobox gene, Ziro3, in the midline axial structures and central nervous system. *Mech. Dev.* **87**, 165-168.
- Trevarrow, B., Marks, D. L. and Kimmel, C. B.** (1990). Organization of hindbrain segments in the zebrafish embryo. *Neuron* **4**, 669-679.
- Varga, Z. M., Amores, A., Lewis, K. E., Yan, Y. L., Postlethwait, J. H., Eisen, J. S. and Westerfield, M.** (2001). Zebrafish smoothed functions in ventral neural tube specification and axon tract formation. *Development* **128**, 3497-3509.
- Westerfield, M.** (2000). *The Zebrafish Book*. Eugene, OR: University of Oregon Press.
- Wichterle, H., Lieberam, I., Porter, J. A. and Jessell, T. M.** (2002). Directed differentiation of embryonic stem cells into motor neurons. *Cell* **110**, 385-397.
- Wolff, C., Roy, S. and Ingham, P. W.** (2003). Multiple muscle cell identities induced by distinct levels and timing of hedgehog activity in the zebrafish embryo. *Curr. Biol.* **13**, 1169-1181.
- Zhou, Q. and Anderson, D. J.** (2002). The bHLH transcription factors OLIG2 and OLIG1 couple neuronal and glial subtype specification. *Cell* **109**, 61-73.
- Zhou, Q., Choi, G. and Anderson, D. J.** (2001). The bHLH transcription factor Olig2 promotes oligodendrocyte differentiation in collaboration with Nkx2.2. *Neuron* **31**, 791-807.
- Zhou, Q., Wang, S. and Anderson, D. J.** (2000). Identification of a novel family of oligodendrocyte lineage-specific basic helix-loop-helix transcription factors. *Neuron* **25**, 331-343.